

# EIT analogs using orthogonally polarized modes of a single whispering-gallery microresonator

A. T. Rosenberger\*

Department of Physics, Oklahoma State University, Stillwater, OK 74078-3072

## ABSTRACT

The throughput of a single fiber-coupled whispering-gallery microresonator, such as a fused-silica microsphere, can exhibit behavior analogous to electromagnetically induced transparency and absorption (EIT, EIA). These effects enable slow and fast light, respectively, in the form of pulse delay or advancement. Two different methods can be used to realize this behavior; in both methods, the key feature is the use of two coresonant orthogonally polarized whispering-gallery modes of very different quality factor ( $Q$ ). The first method relies on intracavity cross-polarization coupling when only one mode is driven, and the second method uses a simple superposition of orthogonal throughputs (in the absence of intracavity cross-polarization mode coupling) when the two modes are simultaneously driven. We refer to the behavior observed using the first method as coupled-mode induced transparency and absorption (CMIT, CMIA), and the behavior of the second method as coresonant polarization induced transparency and absorption (CPIT, CPIA). In both cases, polarization-sensitive detection of the throughput is used, and the EIT/EIA analog features are observed on the same polarization component as that of the linearly polarized input. Some predictions of a numerical model of these processes are presented here. In addition to a discussion of these predictions, which assume conditions accessible to experiment, some experimental results are briefly described.

**Keywords:** whispering-gallery modes, microresonator, induced transparency, pulse delay, slow light, coresonance

## 1. INTRODUCTION

Mode coupling is a feature of many different physical systems. A student's first exposures to the phenomenon are usually through the appearance of normal modes in classical coupled oscillators and level splitting in the quantum double square well. Interaction between modes requires the near-coincidence of resonance frequencies or of energy levels, but this is not sufficient to guarantee coupling. For example, in the Stark and Zeeman effects in atoms, where different levels shift at different rates with increasing applied field, levels will cross if they do not interact, but an anticrossing (or avoided crossing) will be observed if coupling results in level splitting. More sophisticated examples include electromagnetically induced transparency (EIT), which results from coupling of transitions between dressed atomic states and serves as an illustration of how useful the effect of mode coupling can be.<sup>1</sup>

Another classical manifestation of mode coupling occurs in optical resonators. For example, sub-millimeter dielectric disks, cylinders, spheres, and toroids support whispering-gallery modes (WGMs) in which light circulates around the perimeter by total internal reflection. Modes of two different microresonators can couple evanescently if the resonators are almost in contact. This leads to, for example, coupled-resonator induced transparency (CRIT),<sup>2,3</sup> analogous to EIT. In these systems, coupled-resonator induced absorption (CRIA), analogous to electromagnetically induced absorption (EIA) has also been observed. Both processes are of interest because, in general, induced transparency is accompanied by a spectral region of strong normal dispersion and the possibility of slow light (pulse delay); similarly, induced absorption is often accompanied by strong anomalous dispersion and fast light (pulse advance). In a single WGM microresonator, mode splitting due to backscatter-induced coupling of counterpropagating modes has been observed and studied in detail.<sup>4</sup> In addition, because the WGM spectrum of a typical microresonator is rather dense, it is also possible to have coresonant copropagating modes in a single resonator, either by coincidence or through strain tuning of the WGMs. In this way, crossing<sup>5</sup> and anticrossing<sup>6,7</sup> have been observed in otherwise unmodified microresonators. This is of practical as well as fundamental interest, because it means that many applications that were thought to require coupled resonators might be possible with a single resonator.<sup>7</sup>

\*atr@okstate.edu; phone 1 405 744-6742; fax 1 405 744-6811; physics.okstate.edu/rosenber/index.html

Whispering-gallery microresonators have two orthogonally polarized families of modes, TE (transverse electric) and TM (transverse magnetic). Because the birefringence induced by strain tuning causes the two types of modes to tune at different rates, strain tuning can be used to impose frequency degeneracy between a TE mode and a TM mode, i.e., to bring these copropagating modes into coresonance. We have observed that when this coresonance occurs, sometimes mode splitting due to cross-polarization coupling is observed. Because of the similarity of this coupling of coresonant orthogonally polarized modes in a single resonator to the inter-resonator coupling of coresonant modes of the same polarization, we expect behavior analogous to CRIT and CRIA, which we call CMIT and CMIA, for coupled-mode induced transparency and absorption. We have studied this numerically and experimentally, and some of the model results are presented here.

In the case of CMIT and CMIA, the light incident on the microresonator is typically linearly polarized so as to directly excite only one family of modes, say TE, and the mode coupling effects are observed as a splitting or modification of the shape of the resonant throughput dip (of the same polarization; TM output is then also produced). However, we have recently discovered that if the incident light is linearly polarized at  $45^\circ$  in the TE-TM basis to drive coresonant modes of the two polarizations, analogous effects can be observed in the throughput of the same linear polarization as the incident light – even in the absence of cross-polarization coupling. These will be referred to as coresonant polarization induced transparency and absorption (CPIT, CPIA). Again, we have studied these effects numerically and experimentally, and present here some of the model results.

The simple numerical model used, based on a plane-wave ring cavity, will be described next. Then some results will be shown and discussed.

## 2. MODEL

The experimental system to be modeled is shown in the simplified generic sketch of Fig. 1. Light from a tunable laser is coupled into the WGMs of a microresonator from a tapered fiber tangent to the equatorial plane of the resonator. The input polarization is set to any desired state by a polarization controller, and the throughput is sent through a polarizing beamsplitter and the two orthogonal components are detected; the detection system can be rotated about the fiber axis.

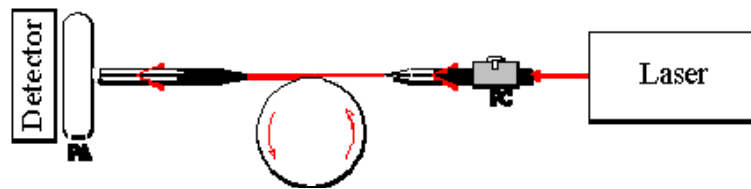


Figure 1. Whispering-gallery microresonator system for investigating induced transparency and absorption analog effects. The laser is tunable; PC is a polarization controller; PA is a polarization analyzer; and the detector is a set of two detectors to measure the powers in two orthogonal polarizations.

The model consists of a plane-wave planar ring resonator with one partially transmitting mirror, similar to that used previously.<sup>8</sup> The polarization state of the input field may be set as desired; the *s-p* polarization basis of the planar ring is equivalent to the TE-TM basis of the microresonator. The output field is resolved into orthogonal linearly polarized components, and the detection basis may be set at any angle with respect to the resonator basis. The output of the model consists of the power spectra of the two throughput components and the phase of each component with respect to the input field. The resonator has two modes (TE and TM), nominally coresonant, but with a frequency detuning that can be adjusted. The two orthogonal modes may have different propagation constants (or effective indices of refraction), but because the input/output coupling takes place at a single point, this difference has only a small effect. Treating the modes as plane waves ignores the transverse profiles of the real microresonator modes. These transverse profiles determine the input/output coupling strengths and the cross-polarization coupling strength; in the model, these coupling strengths are treated as adjustable parameters. Each mode has two losses, the output coupling and intrinsic loss; these are parameters in the model, adjusted indirectly by giving the values (in the absence of cross-polarization coupling) of the quality factor  $Q$  of each mode (determines total loss), of the depth of each mode's resonance dip (determines ratio of losses), and of the coupling regime (allows determination of each loss independently). The coupling regimes are overcoupled (coupling loss greater), undercoupled (intrinsic loss greater), and critical (losses equal).

Cross-polarization coupling between the intracavity circulating TE and TM modes is treated as a cross-polarization scattering near the input/output coupling point.<sup>9</sup> This is very similar to coupling of counterpropagating modes by backscattering, except that in the case of copropagating modes of orthogonal polarization having different effective indices, the scattering must be assumed to take place at a single point. The actual cross-polarization coupling process may be due to polarization rotation of the circulating light, due, for example, to a north-south asymmetry of the slightly prolate spheroidal microresonator. However, there is almost no difference between our model and an existing model for polarization rotation in a resonator.<sup>10,11</sup> Our model has a scattering probability (per round trip) parameter that can be adjusted, or turned off to eliminate cross-polarization coupling.

One other feature of the model is that it calculates the response of the resonator to a Gaussian pulse when the corresponding envelope is imposed on the input field amplitude. For either mode, the circulating intracavity field depends in part on the intracavity field one round-trip earlier; this dependence may be cast as a difference equation, and then since the round-trip time is much shorter than any possible response of the system (high  $Q$  implies a cavity decay time consisting of tens of thousands of round trips), the difference equations are converted to a coupled set of differential equations that can be solved to find the pulse response. Typically, the input pulse width (FWHM) is chosen to be approximately  $0.441/\Delta\nu_{\min}$ , where  $\Delta\nu_{\min}$  is the linewidth of the higher- $Q$  mode, so that the pulse bandwidth equals the linewidth of the higher- $Q$  mode.

### 3. RESULTS

Some typical results of the model are presented in this section. In all cases, the parameter values chosen are experimentally realistic. For example, experimental observations of cross-polarization coupling have shown that a typical coupling strength (effective scattering probability per round trip) is a few times  $10^{-8}$ ; this is at least an order of magnitude larger than a typical backscattering strength. In addition,  $Q$  values of a few times  $10^8$  are routinely achievable in some WGMs of a fused-silica microsphere. In all of the results reported here, the TE and TM modes are assumed to be coresonant; they are labeled 1 and 2, where 1 can be TE or TM and 2 is the other. In all cases  $Q_1 \ll Q_2$ , and the wavelength is taken to be 1550 nm. Each of Figs. 2-7 consists of three parts: (a) is the throughput spectrum of the input polarization component, (b) is the dispersion, specifically the phase of the throughput relative to the input, and (c) shows the input pulse, whose bandwidth is centered at the resonant frequency, and the throughput pulse.

#### 3.1 CMIT/CMIA

In these cases (Figs. 2 and 3), the input light is polarized along the 1 axis, so that mode 1 is driven and mode 2 is excited only by cross-polarization coupling. The figures pertain to the throughput of mode 1's polarization. An example of coupled-mode induced transparency is shown in Fig. 2. Mode 1 is overcoupled, mode 2 is undercoupled. The quality factors of the two modes in the absence of cross-polarization coupling are  $Q_1 = 8 \times 10^6$ ,  $Q_2 = 1.98 \times 10^8$ . The fractional dip depths of the two modes in the absence of cross-polarization coupling are  $M_1 = 0.96$ ,  $M_2 = 0.93$ . The cross-polarization coupling strength is  $T_s = 5 \times 10^{-8}$ . Because the transparency feature doesn't come all the way back up to 1.0, the pulse is attenuated; it is also broadened somewhat, indicating that the region of high dispersion is somewhat narrower than the linewidth of mode 2.

Figure 3 shows coupled-mode induced absorption. The parameters are the same as for CMIT above, except for these:  $M_1 = 0.36$ ,  $M_2 = 0.53$ ,  $T_s = 6.3 \times 10^{-9}$ . In this case there is anomalous dispersion on resonance and the pulse is slightly advanced, although attenuated.

#### 3.2 CPIT/CPIA

In these examples, the input light is linearly polarized at  $45^\circ$ , so that both modes are driven with equal input power. The throughput in Figs. 4-6 is the same polarization as the input, specifically, a symmetric linear superposition of the modes' throughput fields. In all three figures,  $Q_1 = 5 \times 10^6$  and  $Q_2 = 1 \times 10^8$ . In contrast to the conditions of Section 3.1, there is no cross-polarization coupling in Figs. 4 and 5. For the coresonant polarization induced transparency shown in Fig. 4, both modes are overcoupled, and  $M_1 = M_2 = 0.05$ . The example of coresonant polarization induced absorption of Fig. 5 has both modes undercoupled and  $M_1 = 0.31$ ,  $M_2 = 0.72$ . Figure 6 is the same as Fig. 4, except that  $T_s = 5 \times 10^{-8}$ , showing the effect of cross-polarization coupling on CPIT.

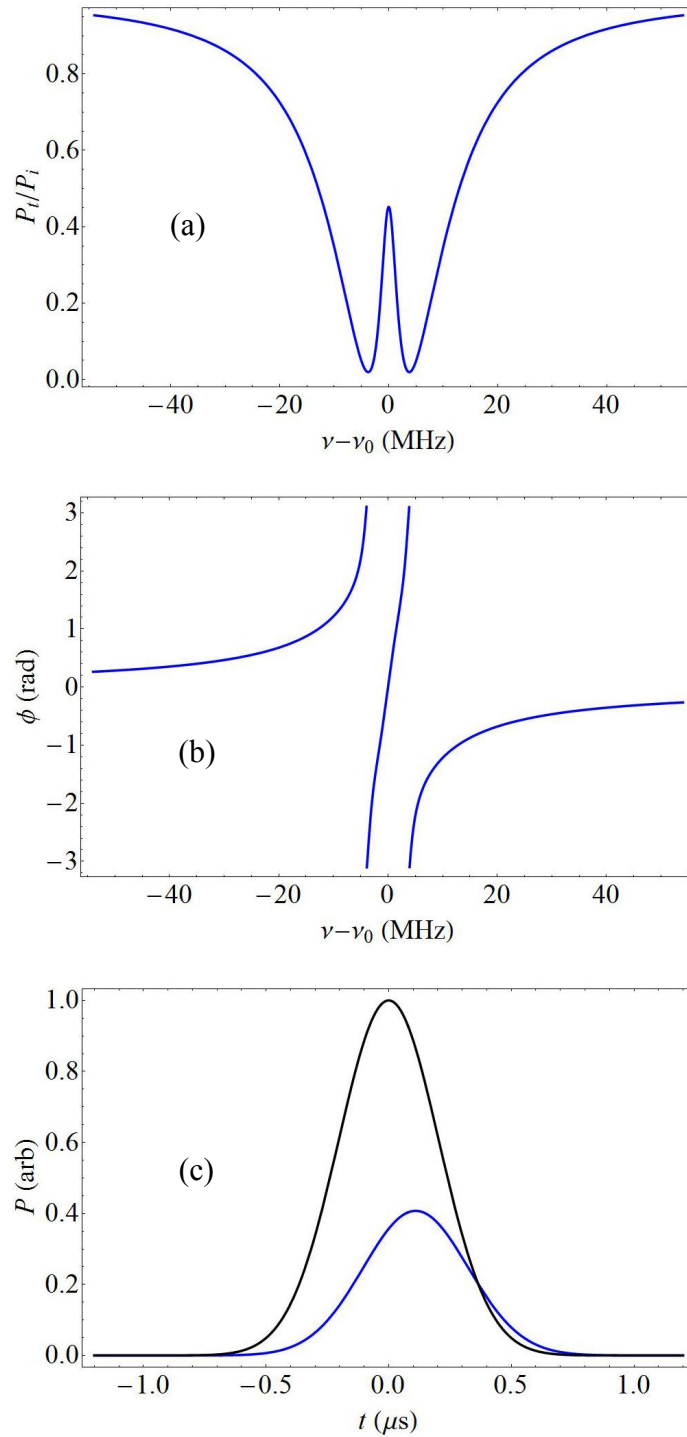


Figure 2. Coupled-mode induced transparency. (a) Throughput spectrum of the input polarization component, driving mode 1. (b) Phase shift of the throughput field relative to the input field. (c) Input Gaussian pulse (amplitude 1, centered at  $t = 0$ ), and throughput pulse.

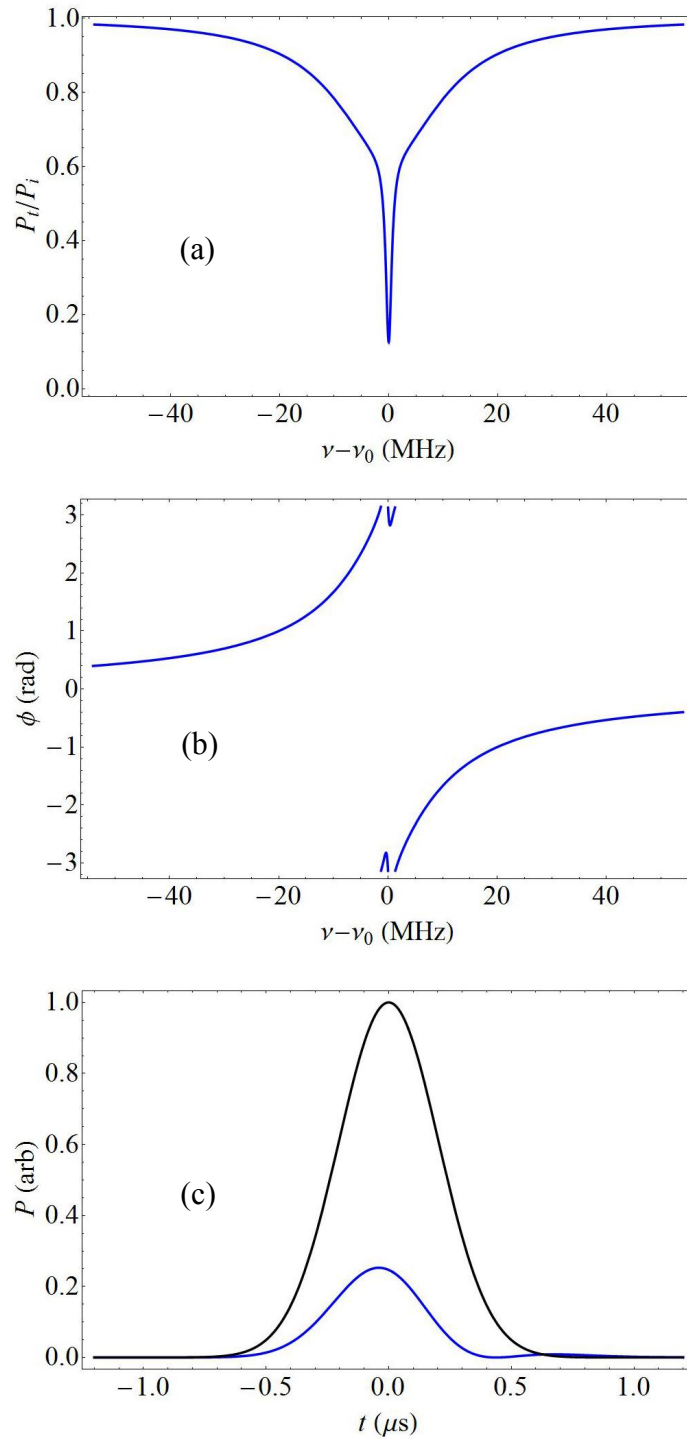


Figure 3. Coupled-mode induced absorption. (a) Throughput spectrum of the input polarization component, driving mode 1. (b) Phase shift of the throughput field relative to the input field. (c) Input Gaussian pulse (amplitude 1, centered at  $t = 0$ ), and throughput pulse.

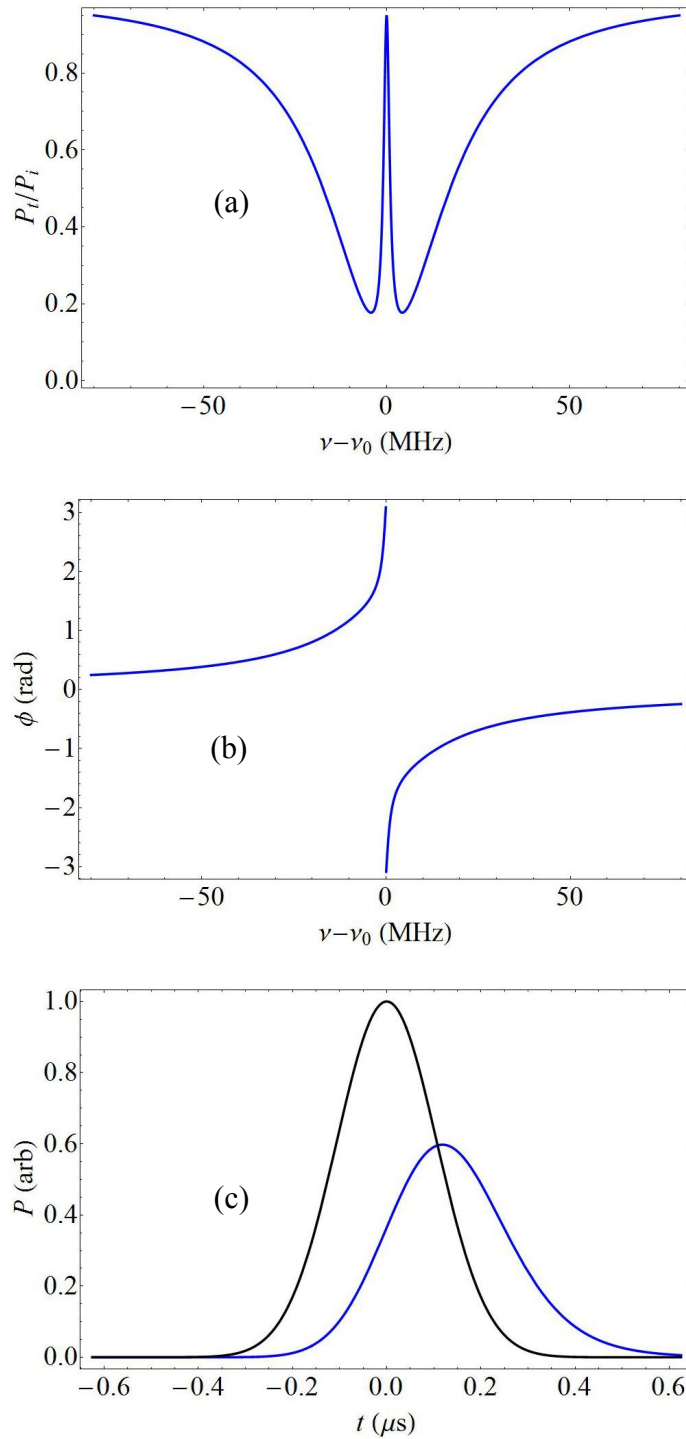


Figure 4. Coresonant polarization induced transparency. (a) Throughput spectrum of the input polarization component at  $45^\circ$ , driving both modes. (b) Phase shift of the throughput field relative to the input field. (c) Input Gaussian pulse (amplitude 1, centered at  $t = 0$ ), and throughput pulse.

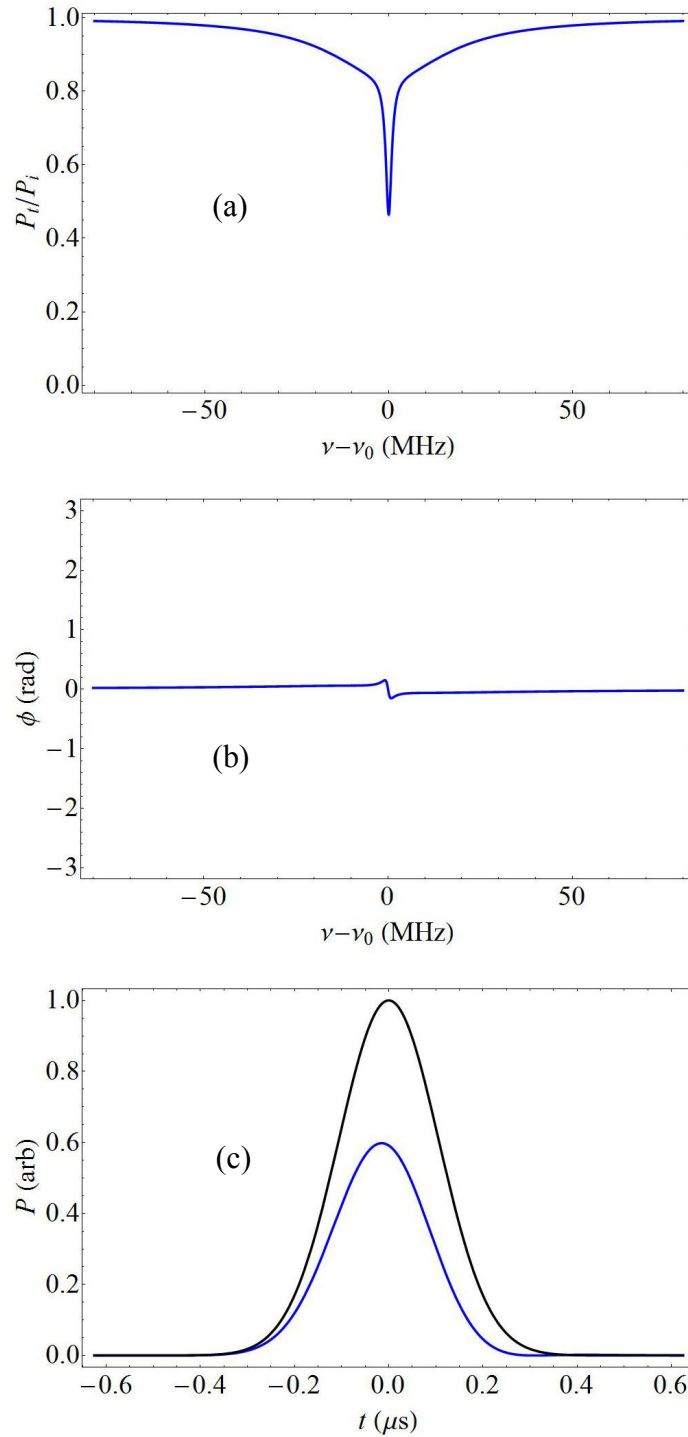


Figure 5. Coresonant polarization induced absorption. (a) Throughput spectrum of the input polarization component at  $45^\circ$ , driving both modes. (b) Phase shift of the throughput field relative to the input field. (c) Input Gaussian pulse (amplitude 1, centered at  $t = 0$ ), and throughput pulse.

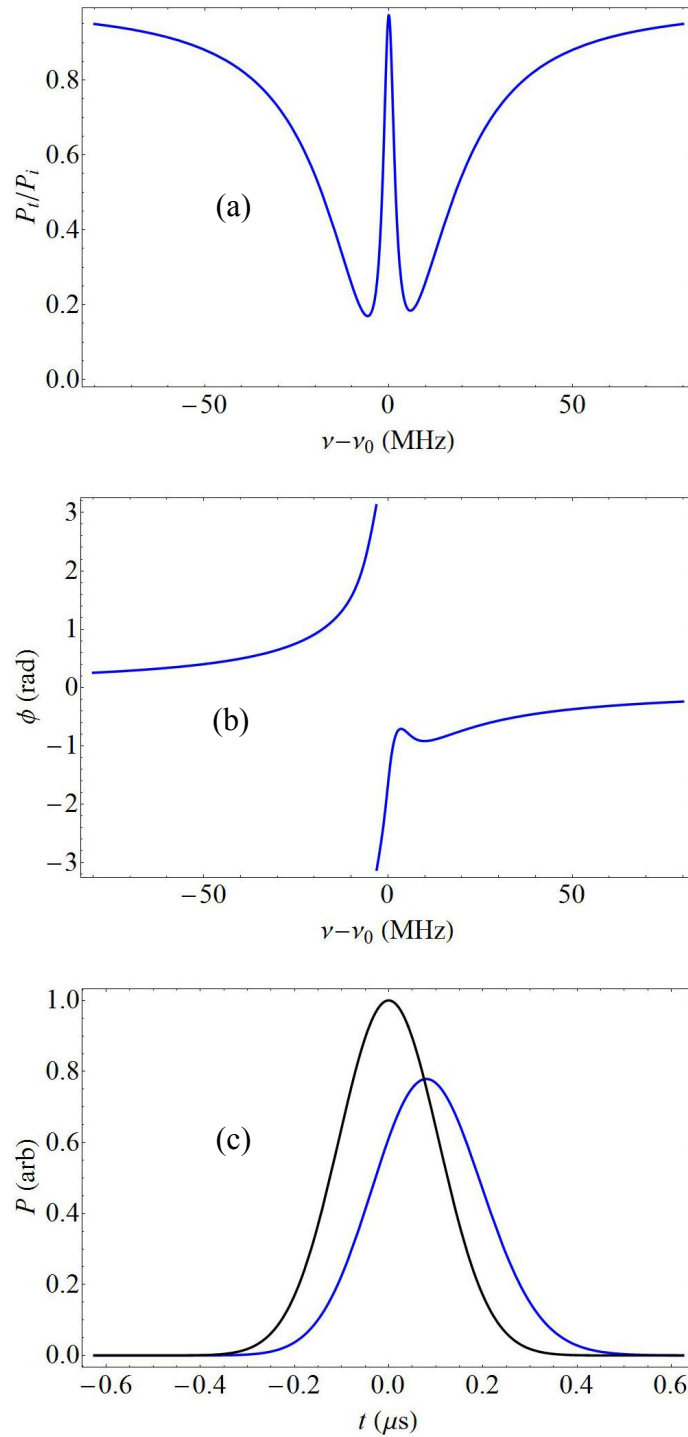


Figure 6. Coresonant polarization induced transparency, as in Fig. 4, but with cross-polarization coupling. (a) Throughput spectrum of the input polarization component at  $45^\circ$ , driving both modes. (b) Phase shift of the throughput field relative to the input field. (c) Input Gaussian pulse (amplitude 1, centered at  $t = 0$ ), and throughput pulse.

### 3.3 Other effects

The behavior of a single overcoupled mode with  $Q = 1.98 \times 10^8$  and  $M = 0.05$  is shown in Fig. 7 for comparison.

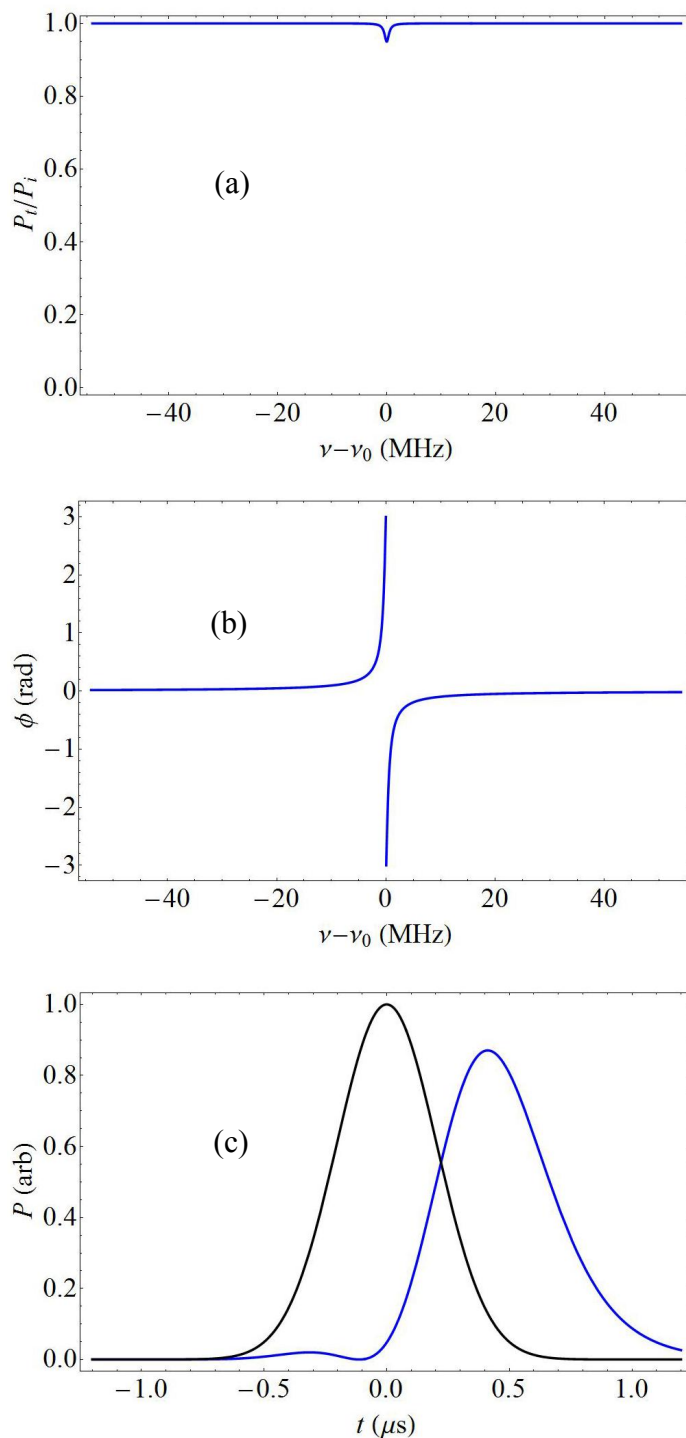


Figure 7. Response of a single driven mode. (a) Throughput spectrum. (b) Phase shift of the throughput field relative to the input field. (c) Input Gaussian pulse (amplitude 1, centered at  $t = 0$ ), and throughput pulse.

## 4. DISCUSSION

With cross-polarization coupling, an induced transparency feature is observable (CMIT, Fig. 2). It is difficult to get close to 100% transmission with experimentally realistic parameter values, but the large phase change at resonance suggests that further investigation is warranted. In Fig. 2 the delay-bandwidth product is only about 0.1, but that might be improved, and the pulse attenuation might be reduced, by using higher- $Q$  WGMs.

The pulse advancement that is achievable in induced absorption, either with cross-polarization coupling (CMIA, Fig. 3) or without it (CPIA, Fig. 5) is always less than the corresponding induced-transparency-related pulse delays. The advancement-bandwidth products are less than 0.05, and the reduced throughput due to induced absorption always means significant pulse attenuation.

Surprisingly, in the absence of any (cross-polarization) mode coupling, the induced transparency that may be observed (CPIT, Fig. 4) is remarkably better than with mode coupling. The throughput at the center of the transparency feature can approach 100%, the dispersion is large, and so the throughput pulse, though somewhat attenuated and broadened, exhibits a delay-bandwidth product of about 0.3 (in Fig. 4). For this case, it is easy to calculate the theoretical maximum delay-bandwidth product, which is 0.318, so the parameters of Fig. 4 are nearly optimal. Adding a bit of cross-polarization coupling to CPIT, as in Fig. 6, slightly broadens the transparency feature, reducing the pulse broadening; it also distorts the dispersion, reducing the pulse delay. Note that the pulse spectrum in Fig. 6(a) becomes asymmetric; this interesting result is related to the symmetry of the normal modes created by the cross-polarization coupling. When mode splitting is observed, the lower-frequency normal mode is a symmetric combination of TE and TM, and the higher-frequency normal mode is their antisymmetric combination. Since the plotted throughput is at  $45^\circ$ , the throughput is a symmetric combination of TE and TM, and so the lower-frequency throughput minimum is deeper.

Finally, theory predicts that the pulse response to a single overcoupled mode (Fig. 7) should have a maximum delay-bandwidth product of 0.637. The throughput pulse seen in Fig. 7 has a delay-bandwidth product of 0.44. With strong overcoupling (shallow dip), the pulse attenuation can also be very small. This configuration, however, loses the frequency-filtering effect of the transparency spike seen in Fig. 4. Related to this behavior is an effect observed in CPIT; there, the pulse delay is tunable by varying the angle of the polarization axis of the linearly polarized input light and always detecting that same component in the throughput. With an angle of  $0^\circ$ , the response reduces to that of the lower- $Q$  overcoupled mode, and with an angle of  $90^\circ$ , the response becomes that of the higher- $Q$  overcoupled mode.

We have observed experimental throughput spectra like those shown in the (a) parts of Figs. 2-7: CMIT, CMIA, CPIT, CPIA, and the effect of cross-polarization coupling on CPIT. A widely tunable semiconductor laser was used, and its tuning range allows us to search for accidentally coresonant modes, but we have also used strain tuning to enforce coresonance and to adjust the frequency detuning of the modes from each other. Some of these throughput spectra have been fitted using our model and experimentally determined parameter values. The cross-polarization coupling strength and the detuning are treated as free parameters for fitting, and this is how typical values of  $T_s$  have been determined. These results will be published elsewhere.

## 5. CONCLUSIONS

EIT (and EIA) analog effects have been demonstrated to be observable using a single resonator that has coresonant TE and TM whispering-gallery modes, not only with but also without cross-polarization mode coupling. Coupled-mode induced transparency is of potential interest for applications, but suffers from the drawback that the coupling strength is not easily controllable. The TE-TM detuning is easily controlled, however; this capability may be quite useful and is deserving of further study. The occurrence of cross-polarization coupling can be problematic if the throughput is not polarization-resolved, but with polarization-sensitive detection, the effects described here become not only observable, but potentially important for applications such as pulse delay.

The effects observed without mode coupling, in the coresonant polarization induced transparency case, are more dramatic and allow for more control. Some near analogs to this effect have been reported.<sup>12,13</sup> It will be interesting to find other analogs in atomic systems or in other classical optical devices such as photonic-crystal waveguide-resonator systems. CPIT and CPIA should also be observable in microring resonators and even in macroscopic multimirror ring cavities, taking advantage of the polarization dependence of the reflectivity of high-reflection coatings.

The EIT analog effects reported here might also be useful for application in areas such as chemical sensing, either absorption sensing or dispersion sensing through frequency shifts. It would also be interesting to investigate the effect on these various processes of having (subthreshold) gain in the microresonator. Experimental studies of pulse response are planned for the near future.

## ACKNOWLEDGMENTS

The author would like to thank his current and former graduate students who contributed to this work, especially to the experimental observation and study of some of the effects described here. Particular thanks go to Elijah Dale, Erik Gonzales, and Khoa Bui; others more peripherally involved include Deepak Ganta, Gregorio Martinez, and Razvan Stoian. Some of this work was made possible by support from the National Science Foundation through Grant Number ECCS-0601362, and from the Oklahoma Center for the Advancement of Science and Technology through Grant Number AR072-066.

## REFERENCES

- [1] Fleischhauer, M., Imamoglu, A., and Marangos, J. P., "Electromagnetically induced transparency: Optics in coherent media," *Rev. Mod. Phys.* 77, 633-673 (2005).
- [2] Smith, D. D., Chang, H., Fuller, K. A., Rosenberger, A. T., and Boyd, R. W., "Coupled-resonator-induced transparency," *Phys. Rev. A* 69, 063804 (2004).
- [3] Naweed, A., Farca, G., Shopova, S. I., and Rosenberger, A. T., "Induced Transparency and Absorption in Coupled Whispering-Gallery Microresonators," *Phys. Rev. A* 71, 043804 (2005).
- [4] Kippenberg, T. J., Spillane, S. M., and Vahala, K. J., "Modal coupling in traveling-wave resonators," *Opt. Lett.* 27, 1669-1671 (2002).
- [5] Savchenkov, A. A., Matsko, A. B., Ilchenko, V. S., Strekalov, D., and Maleki, L., "Direct observation of stopped light in a whispering-gallery-mode microresonator," *Phys. Rev. A* 76, 023816 (2007).
- [6] von Klitzing, W., Long, R., Ilchenko, V. S., Hare, J., and Lefèvre-Seguin, V., "Tunable whispering gallery modes for spectroscopy and CQED experiments," *New Journal of Physics* 3, 14.1-14.14 (2001).
- [7] Carmon, T., Schwefel, H. G. L., Yang, L., Oxborrow, M., Stone, A. D., and Vahala, K. J., "Static Envelope Patterns in Composite Resonances Generated by Level Crossing in Optical Toroidal Microcavities," *Phys. Rev. Lett.* 100, 103905 (2008).
- [8] Rosenberger, A. T., "Analysis of whispering-gallery microcavity-enhanced chemical absorption sensors," *Opt. Express* 15, 12959-12964 (2007).
- [9] Rubin, J. T., and Deych, L., "*Ab initio* theory of defect scattering in spherical whispering-gallery-mode microresonators," *Phys. Rev. A* 81, 053827 (2010).
- [10] Melloni, A., Morichetti, F., and Martinelli, M., "Polarization conversion in ring resonator phase shifters," *Opt. Lett.* 29, 2785-2787 (2004).
- [11] Morichetti, F., Melloni, A., and Martinelli, M., "Effects of Polarization Rotation in Optical Ring-Resonator-Based Devices," *J. Lightwave Technol.* 24, 573-585 (2006).
- [12] Zeldovich, B. Ya., and Soileau, M. J., "Bi-frequency pendulum on a rotary platform: modeling various optical phenomena," *Physics-Uspekhi* 47, 1239-1255 (2004).
- [13] Verslegers, L., Yu, Z., Ruan, Z., Catrysse, P. B., and Fan, S., "From Electromagnetically Induced Transparency to Superscattering with a Single Structure: A Coupled-Mode Theory for Doubly Resonant Structures," *Phys. Rev. Lett.* 108, 083902 (2012).